Therapeutic Potential of Human Induced Pluripotent Stem Cells in Experimental Stroke

Article *in* Cell Transplantation · October 2012

DOI: 10.3727/096368912X657314 · Source: PubMed

Cell Transplantation, Vol. 22, pp. 000–000, 2013
Printed in the USA.

0963-6897/13 $90.00 + .00
DOI: http://dx.doi.org/10.3727/096368912X657314
E-ISSN 1555-3892
www.cognizantcommunication.com

Therapeutic Potential of Human Induced Pluripotent Stem Cells in Experimental Stroke

Da-Jeong Chang,*[1] Nayeon Lee,*[1] In-Hyun Park,†‡[1] Chunggab Choi,* Iksoo Jeon,* Jihye Kwon,* Seung-Hun Oh,* Dong Ah Shin,§ Jeong Tae Do,* Dong Ryul Lee,* Hyunseung Lee,¶ Hyeyoung Moon,¶ Kwan Soo Hong,¶ George Q. Daley,† and Jihwan Song*

*CHA Stem Cell Institute, Department of Biomedical Science, CHA University, Seoul, Korea
†Department of Biological Chemistry and Molecular Pharmacology, Harvard Medical School, Boston, MA, USA
‡Department of Genetics, Yale University School of Medicine, New Haven, CT, USA
§Department of Neurosurgery, Yonsei University College of Medicine, Seoul, Korea
¶Division of Magnetic Resonance, Korea Basic Science Institute, Ochang, Korea

Ischemic stroke mainly caused by middle cerebral artery occlusion (MCAo) is a major type of stroke, but there are currently very limited therapeutic options for its cure. Neural stem cells (NSCs) or neural precursor cells (NPCs) derived from various sources are known to survive and improve neurological functions when they are engrafted in animal models of stroke. Induced pluripotent stem cells (iPSCs) generated from somatic cells of patients are novel cells that promise the autologous cell therapy for stroke. In this study, we successfully differentiated iPSCs derived from human fibroblasts into NPCs and found their robust therapeutic potential in a rodent MCAo stroke model. We observed the significant graft-induced behavioral recovery, as well as extensive neural tissue formation. Animal MRI results indicated that the majority of contralaterally transplanted iPSC-derived NPCs migrated to the peri-infarct area, showing a patho-tropism critical for tissue recovery. The transplanted animals exhibited the significant reduction of stroke-induced inflammatory response, gliosis and apoptosis, and the contribution to the endogenous neurogenesis. Our results demonstrate that iPSC-derived NPCs are effective cells for the treatment of stroke.

Key words: Stroke; Induced pluripotent stem cells (iPSCs); Behavioral recovery; Endogenous neurogenesis

INTRODUCTION

Ischemic stroke mainly caused by middle cerebral artery occlusion (MCAo) represents the major type of stroke, which leads to the death of multiple neuronal cell types, as well as astrocytes, oligodenderocytes, and endothelial cells in the brain (20,33). After stroke, spontaneous recovery may occur to varying degrees, but most patients suffer from persistent motor, sensory, or cognitive impairments. Despite extensive research efforts, there are still very limited therapeutic options for stroke-damaged patients. Based on numerous animal transplantation experiments using various cell sources, as well as new observations on the stroke-induced neurogenesis, the action modes of stem cell-based approaches in stroke can be proposed largely in the following ways (20). Firstly, stem cell-derived neural precursor cells (NPCs) can be transplanted to restore damaged neural tissues and circuitry. Secondly, various kinds of stem cells can be injected systemically to achieve neuroprotection and modulation of inflammation. Thirdly, drugs or chemical compounds can be infused to promote neurogenesis from endogenous stem/progenitor cells in the sub-ventricular zone (SVZ).

Clinical trials have been performed using various cell sources, from immortalized human teratocarcinoma cell line to autologous bone marrow-derived mesenchymal stem cells (BM-MSCs) (2,8,17,18,23). Outcomes have been variable with some reports describing no benefit while others have indicated transient clinical improvement (19). More recently, another clinical trial in stroke patients is ongoing by ReNeuron using clonal, conditionally immortalized neural stem cells (NSCs) isolated from human fetal cortex, which were previously shown to ameliorate motor impairments in the rat stroke model

Received March 3, 2012; final acceptance June 20, 2012. Online prepub date: October 3, 2012.
[1]These authors provided equal contribution to this work.
Address correspondence to Jihwan Song, D.Phil., CHA Stem Cell Institute, Department of Biomedical Science, CHA University, 606-16 Yeoksam 1-dong, Kangnam-gu, Seoul 135-081, Korea. Tel: +82 2 3468 3393; Fax: +82 2 538 4102; E-mail: jsong@cha.ac.kr

(29). In any case, while autologous MSCs provide minimal clinical outcomes, human fetal tissue transplants raise ethical issues and inevitably are genetically dissimilar to the recipient with the associated risk of immune rejection. Therefore, other suitable nonfetal cell source of syngeneic donor tissue with high neurogenic potential would be advantageous.

In this study, we show that an iPSC derived from normal human fibroblasts can form NPCs efficiently. After intrastriatal implantation of these cells into a rodent model of MCAo, the grafted animals exhibit clear functional recovery with neural tissue formation in the damaged brain by the transplanted cells. They also show significant reduction in inflammation, gliosis, and apoptosis, as well as significant contribution to the endogenous neurogenesis, implying that iPSC-derived NPCs have the unique properties of treating stroke using all the several modes of action as described above (20).

MATERALS AND METHODS

Culture and Neuronal Differentiation of 551-8 hiPSCs

We cultured and maintained human iPSCs (Detroit 551-iPS8, called 551-8 hiPSC thereafter) according to the method described previously (26–28). We previously established the 551-8 hiPSC line (26), but its neuronal differentiation has not been studied extensively. As a control, H9 human ES cells (obtained from WiCell, Madison, WI, USA) were used. Neuronal differentiation of iPSCs was induced by coculturing the cells with mouse PA6 stromal cells (obtained from RIKEN Cell Bank, Ibaraki, Japan) as described previously (15). Undifferentiated iPSC colonies were mechanically dissected and transferred onto freshly prepared PA6 cells in differentiation medium (DM-PA6) that consists of Glasgow minimum essential medium (GMEM) containing 10% KO-SR (knockout serum replacement, both Invitrogen, Carlsbad, CA, USA), and 4 days later, the KO-SR in DM-PA6 was replaced by N2 supplements (Invitrogen). In the following 11–13 days, definitive neural rosette-like structures containing neuroepithelial (NE) cells were formed, which were mechanically detached and transferred onto a nonsticky Petri dish (BD Biosciences, San Jose, CA, USA) for suspension culture for 7 days to induce neurosphere formation.

Stable Generation of Neural Precursor Cells (NPCs)

To prepare NPCs for transplantation, we dissociated neurospheres into single cells following treatment with Accutase™ (Chemicon, Temecula, CA, USA) and plated them onto poly L-ornithine (PLO; 15 μg/ml, Sigma, St. Louis, MO, USA)/fibronectin (FN; 1 μg/ml, Sigma)-coated 60 mm^2 tissue culture dishes (BD Biosciences). NPCs were maintained in GMEM supplemented with 1% penicillin, 1% streptomycin (both Welgene, Daegu, Korea), 1% nonessential amino acids, 0.1% β-mercaptoethanol, N2 supplements, and 20 ng/ml basic fibroblast growth factor (bFGF; all Invitrogen).

Differentiation Into Mature Neurons (MNs)

To differentiate iPSCs into mature neurons, we plated neurospheres directly onto PLO/FN-coated dishes in DM supplemented with 20 ng/ml brain-derived neurotrophic factor (BDNF, R&D Systems, Minneapolis, MN, USA) in the absence of bFGF.

Immunocytochemical Analysis

To analyze the marker expression of NPCs and differentiated neuronal cells, we carried out immunocytochemical analyses using the following primary antibodies: octamer-binding transcription factor 4 (OCT4; 1:250, Santa Cruz Biotechnology, Dallas, TX, USA), stage-specific embryonic antigen 4 (SSEA-4; 1:100, Developmental Studies Hybridoma Bank, Iowa City, IA, USA), TRA-1-81 (1:250, Chemicon), human-specific nuclei (hNu; 1:200, Chemicon), human-specific mitochondria (hMito; 1:200, Chemicon), human-specific NESTIN (1:200, Chemicon), sex-determining region Y box 2 (SOX2; 1:200, Chemicon), type III β-tubulin (Tuj1) (1:500, Chemicon), orthodenticle homeobox 2 (OTX2; 1:500, Chemicon), brain factor-1 (BF-1; 1:100, Santa Cruz), microtubule-associated protein 2 (MAP2; 1:200, Chemicon), neuronal nuclei (NeuN; 1:500, Chemicon), γ-aminobutyric acid (GABA; 1:5000, Sigma), glutamic acid decarboxylase 65/67 (GAD65/67; 1:200, Chemicon), dopamine- and cAMP-regulated phosphoprotein, Mr 32 kDa (DARPP-32; 1:100, Cell Signaling Technology, Danvers, MA, USA), tyrosine hydroxylase (TH; 1:1000, Pel-Freez, Rodgers, AR, USA), glial fibrillary acidic protein (GFAP; 1:500, BD Biosciences), oligodendrocyte marker 4 (O4; 1:250, Chemicon), ionized calcium-binding adapter molecule 1 (Iba-1; 1:250, Wako, Osaka, Japan), ED1 [cluster of differentiation 68 (CD68); 1:250, Serotec; Raleigh, NC, USA], doublecortin (DCX; 1:200, Cell Signaling), polysialylated-neural cell adhesion molecule (PSA-NCAM; 1:250, Chemicon), and chemokine (C-X-C motif) receptor 4 (CXCR4; 1:40, R&D Systems). Secondary antibodies used were goat anti-mouse IgG-conjugated Alexa-555 (1:200, Molecular Probes, Eugene, OR, USA), goat anti-rabbit IgG-conjugated Alexa-488 (1:200, Molecular Probes), and goat anti-mouse IgM-conjugated Alexa-555 (1:200, Molecular Probes). Staining patterns were examined and photographed using a confocal laser scanning microscope imaging system (LSM510, Carl Zeiss, Inc., Thornwood, NY, USA).

RNA Isolation and Reverse Transcription-Polymerase Chain Reaction (RT-PCR) Analysis

We isolated total RNA from cells using Trizol RNA extraction method (Gibco, Gaithersburg, MD, USA). cDNA was synthesized using Moloney Murine Leukemia

Table 1. RT-PCR Primers Used in This Study

Gene Name	Forward (F) and Reverse (R) Primer Sequences	Product Size (bp)	Annealing Temp. (°C)	No. Cycles	Gene Bank Accession No.
Oct4	F: 5′-CTGAAGCAGAAGAGGATCAC-3′ R: 5′-GACCACATCCTTCTCGAGCC-3′	366	60	30	NM_002701.4
Nanog	F: 5′-TTCTTGACCGGGACCTTGTC-3′ R: 5′-GCTTGCCTTGCTTTGAAGCA-3′	256	60	30	NM_024865
Sox2	F: 5′-GCTGCAAAAGAGAACACCAA-3′ R: 5′-CTTCCTGCAAAGCTCCTACC-3′	232	59	30	NM_003106
Nestin	F: 5′-TCCAGAAACTCAAGCACCA-3′ R: 5′-AAATTCTCCAGGTTCCATGC-3′	183	59	30	NM_006617
Musashi	F: 5′-ACAGCCCAAGATGGTGACTC-3′ R: 5′-CCACGATGTCCTCACTCTCA-3′	191	59	30	NM_002442
βIII tubulin	F: 5′-ATGAGGGAGATCGTGCACAT-3′ R: 5′-GCCCCTGAGCGGACACTGT-3′	239	59	30	BC000748.2
Map2	F: 5′-GCATATGCGCTGATTCTTCA-3′ R: 5′-CTTTCCGTTCATCTGCCATT-3′	202	59	30	U01828
Bf-1	F: 5′-CTCAGAACTCGCTGGGCAAC-3′ R: 5′-CGTGGGGGAAAAAGTAACTGG-3′	225	59	30	NM_005249
Otx2	F: 5′-CGCCTTACGCAGTCAATGGG-3′ R: 5′-CGGGAAGCTGGTGATGCATAG-3′	618	60	30	AF093138
En-1	F: 5′-CTAGCCAAACCGCTTACGAC-3′ R: 5′-GCAGAACAGACAGACCGACA-3′	358	59	30	NM_001426.3
Darpp-32	F: 5′-CCTGAAGGTCATCAGGCAGT-3′ R: 5′-GGTCTTCCACTTGGTCCTCA-3′	131	50	30	AF464196.1
GAD67	F: 5′-AGCAAACCGTGCAATTCCTC-3′ R: 5′-AAATCGAGGATGACCTGTGC-3′	230	55	30	L16888.1
GFAP	F: 5′-GCAGAGATGATGGAGCTCAATGACC-3′ R: 5′-GTTTCATCCTGGAGCTTCTGCCTCA-3′	266	59	30	BC041765.1
MBP	F: 5′-ATTAGCTGAATTCGCGTGTG-3′ R: 5′-CTCTGAGTGCGCAAGTCTTC-3′	235	59	30	M13577.1
GAPDH	F: 5′-GTCATACCAGGAAATGAGCT-3′ R: 5′-TGACCACAGTCCATGCCATC-3′	422	60	30	BC083511.1

Oct4, octamer-binding transcription factor 4; Sox2, sex-determining region Y box 2; Map2, microtubule-associated protein 2; Bf-1, brain factor-1; Otx2, orthodenticle homeobox 2; En-1, engrailed-1; Darpp-32, dopamine- and cAMP-regulated phosphoprotein, Mr 32 kDa; GAD67, glutamate decarboxylase 67; GFAP, glial fibrillary acidic protein; MBP, myelin basic protein; GAPDH, glyceraldehyde 3-phosphate dehydrogenase.

Virus M-MLV reverse transcriptase (Promega, Madison, WI, USA) at 42°C for 1 h. PCR amplification was performed using Taq polymerase according to the manufacturer's instructions (Intron Biotechnology, Kyungki-Do, Korea). Primer sequences, number of cycles, annealing temperatures are described in Table 1. The housekeeping gene glyceraldehyde-3-phosphate dehydrogenase (GAPDH) was used as an internal loading control.

MCAo Animal Model and Cell Transplantation

We carried out animal experiments in accordance with the CHA University IACUC (Institutional Animal Care and Use Committee; IACUC090012). MCAo was induced according to the method of Longa (21) using adult male Sprague–Dawley rats (Orient, Seoul, Korea), weighing 270–300 g. Blunt-ended monofilament (4–0, Ethicon, Livingston, Scotland, UK) was inserted approximately 19 mm from the carotid bifurcation into the internal carotid artery to occlude middle cerebral artery (MCA) for 90 min, after which monofilament was carefully removed. In order to determine and select the appropriate stroke animal models, we employed the acute neurological assessment during the first 24 h after 90 min of MCAo, which include forelimb and hindlimb placement (5) and circling behavior (3). Animals scored 3 points or lower (normal: 5 points) were used for transplantation experiments. At 7 days post-MCAo induction, we injected a total of 10 rats with 2 µl of 551-8 hiPSC-derived NPCs (100,000 cells/µl) into the contralateral side of the infarct region using a Hamilton syringe (Reno, NV, USA), targeting the following coordinates: AP +1.0 mm, ML +3.0 mm, and DV –5.0 mm from the Bregma. In the control group ($n = 10$), 2 µl of suspension medium (GMEM) were injected in parallel. For animal magnetic resonance imaging (MRI) experiments ferumoxide (Feridex®) (Taejoon Pharm, Seoul, Korea) and protamine sulfate (Sigma) were initially prepared at a

concentration of 10 μg/ml in DMEM (Dulbecco's modified Eagle's medium, Invitrogen) without serum, which were mixed for 30 min at room temperature and subsequently added at an equal volume to the culture medium containing the cells for 12–16 h at 37°C. Transplanted animals were immunosuppressed with cyclosporine A (10 mg/kg, Sigma) intraperitoneally 24 h before transplantation and then everyday for up to 8 weeks.

Behavioral Tests

To determine that MCAo models were properly made and to evaluate whether rats recovered functionally following cell transplantation, we performed rotarod test (13), stepping test (24), and modified neurological severity score (mNSS) test (30) every week, and apomorphine-induced rotation test (32) every 2 weeks following transplantation. To determine the baseline scores, each test was performed 1–3 days prior to transplantation.

Statistical Analysis

We performed statistical analyses on the behavior data using the Statistical Analysis System (Enterprise 4.1; SAS, Seoul, Korea) on a CHA University mainframe computer. Performance measures were analyzed using the PROC MIXED program, a linear mixed models procedure for conducting repeated measures analyses of both normal data. The results are presented as the mean ± SEM (standard error of mean). A value of $p < 0.05$ was regarded as significant.

MRI Detection of Transplanted Cells

We employed a 4.7T Bio Spec (Bruker, Ettlingen, Germany) for animal MRI analysis using T2- and T2*-weighted imaging techniques. The MRI setting and detection methods were the same as previously described (16). To detect the Feridex®-labeled 551-8 hiPSC-derived NPCs, Prussian blue staining was carried out by incubating the cells with a mixture of 4% potassium ferrocyanide (Sigma) and 20% hydrochloric acid (Sigma) for 30 min at room temperature, followed by immunohistochemical staining using antibodies against human-specific nuclei or mitochondria, in combination with markers of interest. Prior to transplantation, we confirmed that the cells were completely labeled with Feridex®, as demonstrated by the Prussian blue staining pattern.

Immunohistochemical Analysis

For immunohistochemical analysis, we sacrificed the rats at 8 weeks posttransplantation, perfused, and fixed their brains with 4% paraformaldehyde (Sigma). Frozen coronal sections (40 μm) were prepared using a cryostat (Microm, Walldorf, Germany). Antibodies used for immunohistochemistry were the same as described in immunocytochemical analysis (see above). To detect the endogenous stem cells, we injected 5′-bromo-2′-deoxyuridine (BrdU) (50 mg/kg, Sigma) intraperitoneally three times at 12-h intervals prior to sacrifice. BrdU-positive cells were detected by immunohistochemistry using an antibody against BrdU (1:500, BD Biosciences) following denaturation of DNA using 1M HCl for 30 min at 45°C.

Terminal Deoxynucleotidyl Transferase dUTP Nick End Labeling (TUNEL) Assay

To detect apoptotic cells, frozen sections were stained using In Situ Cell Detection Kit according to the manufacturer's instructions (Roche, Indianapolis, IN, USA). All sections were counterstained with 4′,6-diamidino-2-phenylindole (DAPI; Roche). The number of TUNEL-positive cells were counted using Image J (NIH, Bethesda, MD, USA) and processed for statistical analysis.

RESULTS AND DISCUSSION

Neuronal Differentiation of 551-8 Cells

We have previously isolated an iPSC line from Detroit 551 human fibroblasts (551-iPS8, called 551-8 hiPSCs thereafter) by retroviral infection of four reprogramming factors [OCT4, SOX2, Krüppel-like factor 4 (KLF4),

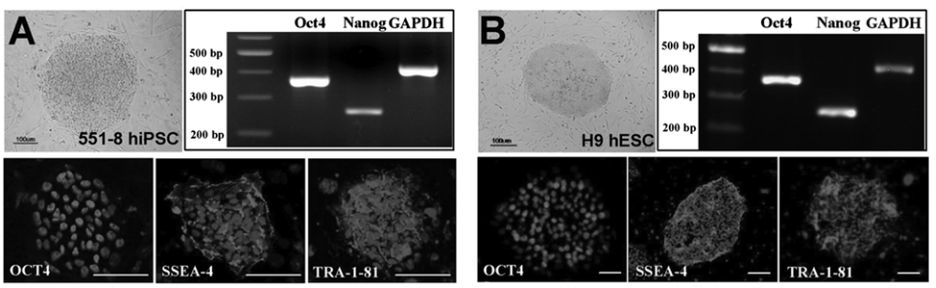

Figure 1. Comparison of undifferentiated 551-8 hiPSCs and H9 ESCs. Comparison of undifferentiated 551-8 human induced pluripotent stem cells (hiPSCs) (A) with H9 human embryonic stem cells (ESCs) (B), in terms of morphology, semiquantitative RT-PCR [octamer binding transcription factor 4 (Oct4) and Nanog], and immunocytochemical [OCT4, stage-specific embryonic antigen (SSEA-4) and TRA-1-81] analyses. Scale bar: 100 μm. GAPDH, glyceraldehyde 3-phosphate dehydrogenase.

and V-myc myelocytomatosis viral oncogene homolog (MYC)] (25). 551-8 cells showed very similar properties with H9 hESCs, in terms of hESC-like morphology, and pluripotency marker expression by semiquantitative RT-PCR and immunocytochemical analyses (Fig. 1A, B), confirming their pluripotency. In order to test the therapeutic effect of hiPSCs for stroke, we initiated the neuronal differentiation of 551-8 iPSCs and H9 hESCs (Fig. 2A). Our differentiation protocol involves the maintenance of the undifferentiated H9 or 551-8 cells on mouse embryonic fibroblasts (MEFs) (Stage 1), coculture with PA6 stromal cells (Stage 2), the isolation of neural rosette-like structure (Stage 3, Fig. 2B), and the neurosphere formation (Stage 4, Fig. 2C). Afterwards, neurospheres were either dissociated into single cells to make neural precursor cells (NPCs) (Stage 5-NP, Fig. 2D) for transplantation or further differentiated into mature neurons (Stage 5-MN, Fig. 2E). Following the Stage 3 of differentiation, we found that the 551-8 iPSCs and H9 hESCs showed the difference in their rosette-forming capacity. While more

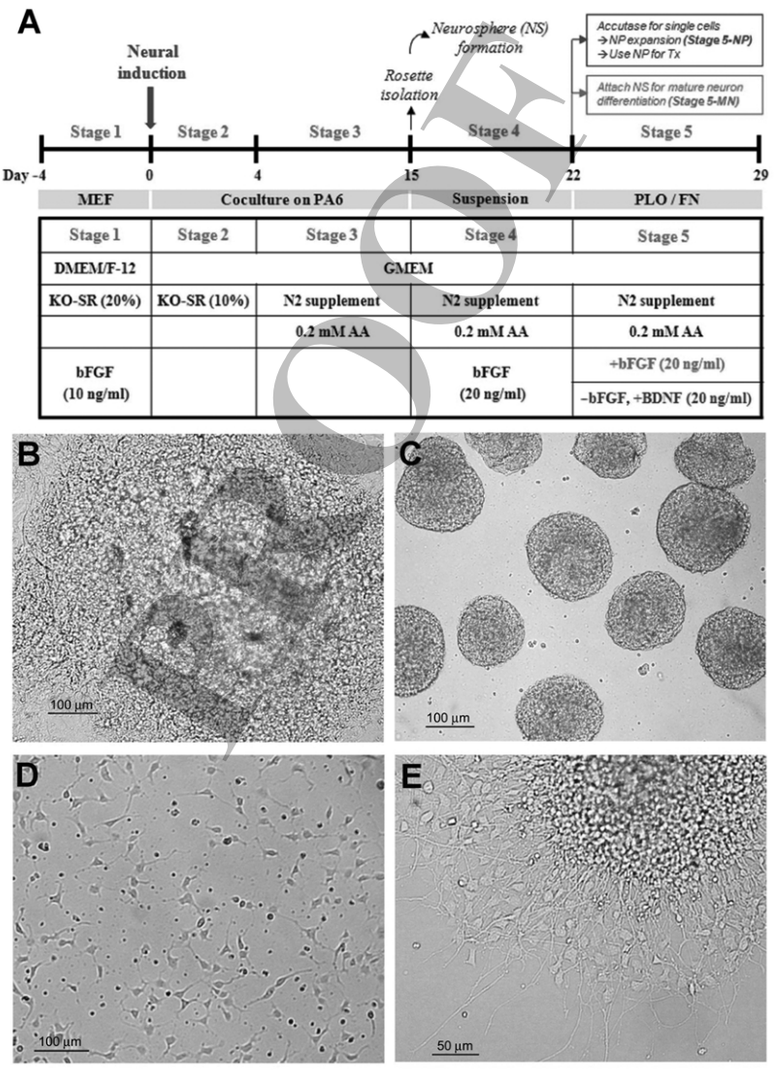

Figure 2. Neuronal differentiation of 551-8 hiPSCs. (A) Experimental scheme showing a step-wise neuronal differentiation procedure. (B) Neural rosette-like structures formed through coculturing 551-8 hiPSCs with mouse PA6 stromal cells (Stage 3, see text for details). (C) Neurospheres (NS) formed though suspension culture of isolated neural rosette-like structures (Stage 4). (D) Neural precursor (NP) cells undergoing expansion as single cells (Stage 5-NP), which were prepared by dissociation of neurospheres using accutase. (E) Differentiated neuronal cells formed from the attached neurospheres (Stage 5-MN). MEF, mouse embryonic fibroblasts; DMEM, Dulbecco's modified Eagle's medium; GMEM, Glasgow minimum essential medium; KO-SR, knockout serum replacement; AA, ascorbic acid; bFGF, basic fibroblast growth factor; BDNF, brain-derived growth factor.

than 80% colonies of H9 cells showed the rosette-like structure, around 20% colonies of 551-8 iPSCs showed the rosette-like structure. The difference may be due to the intrinsic clonal variation among pluripotent stem cells or specific to iPSCs (10,25). A larger number of hESCs and iPSCs will be needed to further investigate the issue involved in the difference in neuronal differentiation (4).

Although the initial rosette-forming efficiency of 551-8 cells was relatively lower than H9 cells, we isolated the rosette-like structures at Stage 3 and further differentiated them into later stages. Interestingly, we found that high levels of NPC markers, such as NESTIN, SOX2, Musashi, were robustly expressed at Stage 5-NPCs in 551-8 iPSCs, comparably as those in H9 cells (Fig. 3A, B). At mature neuronal differentiation stage (Stage 5-MN), we observed that the cultures express markers for various neuronal cell types that include general neurons (Tuj1), mature neurons (MAP2 and NeuN), forebrain/midbrain (Otx2), forebrain (BF-1), medium spiny projection neurons (DARPP-32), GABAergic (GABA and GAD67), and dopaminergic (TH) neurons, as well as markers for astrocytes (GFAP) and oligodendrocytes [O4 and myelin basic protein (MBP)] (Fig. 4A, B). By contrast, markers for pluripotency (Oct4 and Nanog) or midbrain/hindbrain [homeobox protein engrailed-1 (En-1)] were not detectable (Fig. 4B). Taken together, these results indicate that 551-8 iPSCs are highly efficient in completing the neuronal differentiation despite their lower rosette-forming capacity.

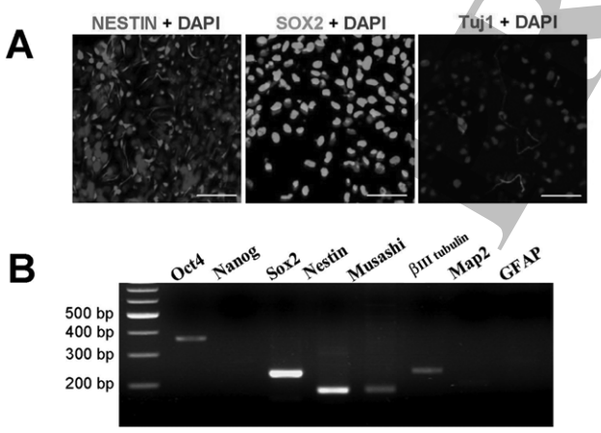

Figure 3. Characterization of 551-8 hiPSC-derived neural precursor cells (Stage 5-NP). (A) Immunocytochemical staining showing high levels of NESTIN and sex-determining region Y box 2 (SOX2) expression and low levels of βIII tubulin (Tuj1) expression. 4′,6-diamidino-2-phenylindole (DAPI) was used for counterstaining the individual cells. (B) Semiquantitative RT-PCR analysis showing the expression of pluripotency markers (i.e., Oct4, Nanog), neural precursor markers (i.e., Sox2, Nestin, Musashi), early and late neuronal markers [βIII tubulin and microtubule-associated protein 2 (Map2), respectively], and an astrocyte marker [glial fibrillary acidic protein (GFAP)]. Scale bar: 50 μm.

Behavioral Improvement Following Transplantation of 551-8 hiPSC-Derived NPCs Into MCAo Animal Models

We next investigated whether the iPSC-derived NPCs (iPSC-NPCs) could exert functional effects after transplantation into a rodent model of ischemic stroke (Fig. 5A). For in vivo studies, we first induced 90-min MCAo and selected appropriate animals by behavioral standards. One week later we grafted 200,000 551-8 hiPSC-NPCs (Stage 5), in a volume of 2 μl, into the striatum of contralateral side of infarct area ($n=10$). In sham control rats ($n=10$), we only injected vehicle (GMEM). We chose the contralateral side, as opposed to ipsilateral side, because our previous MRI study using human bone marrow-derived mesenchymal stem cells (BM-MSCs) demonstrated that most stem cells have the capacity to migrate to the injury site (16). In addition, the ipsilateral injection risks introducing secondary injury to the infarct area, when the Hamilton syringe is inserted into the infarct area, which will inevitably cause tissue damage and inflammatory response. Moreover, the contralateral injection avoids the misinterpretation of MRI results, because the injection site itself can be interpreted as false positive.

To evaluate the functional effects of the grafts, we employed four different behavioral tests (i.e., rotarod, stepping, mNSS, and apomorphine-induced rotation tests). When we followed the transplantation up to 8 weeks, significant behavioral recovery ($p<0.05$) was observed as early as 1 week (in the rotarod test) or 2 weeks (in the staircase, mNSS, and apomorphine-induced rotation tests) (Fig. 5B). Among the tests we employed, we observed more steady and gradual improvements in the rotarod and mNSS tests, compared with stepping and apomorphine-induced rotation tests. In addition to improvement of motor functions, we also observed the improvement of sensory functions in the mNSS test. Taken together, these results strongly indicate that the transplanted 551-8 hiPSC-NPCs contribute to the behavioral improvement in the MCAo stroke animal model.

Formation of Neural Tissues From the Transplanted iPSC-NPCs

After completion of the behavioral tests at 8 weeks, we sacrificed the rats and performed the hisological analysis of the brains. To identify the donor human cells, we used antibodies against human-specific nuclear antigen (hNu) and human mitochondria (hMito) (Fig. 5C). Using confocal microscopy and double immunostaining, we found that some transplanted 551-8 hiPSC-derived cells were still NESTIN-positive neural precursors. Importantly, a large number of the surviving human cells formed MAP2- and NeuN-positive mature neurons. They also formed medium spiny projection neurons (MSN), essential for striatal function. Moreover, we found that some neurons expressed markers for GABAergic (GAD65/67) and dopaminergic (TH) neurons. We also observed small populations of

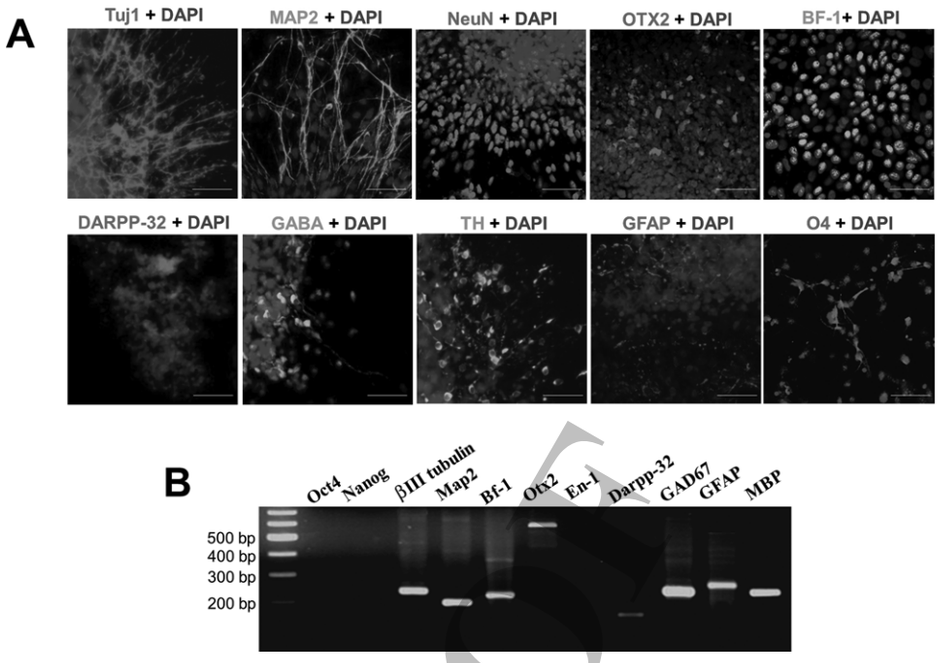

Figure 4. Characterization of 551-8 hiPSC-derived mature neurons (Stage 5-MN). (A) Immunocytochemical staining showing the expression of markers for early (Tuj1), mature (MAP2 and NeuN), forebrain/midbrain (OTX2), forebrain (BF-1), medium spiny projection (DARPP-32), GABAeric (GABA), dopaminergic (TH) neurons, and astrocytes (GFAP), and oligodendrocytes (O4). (B) Semiquantitative RT-PCR analysis showing the expression of markers for pluripotency (i.e., Oct4, Nanog), early and late neurons (Tuj1 and Map2, respectively), forebrain (Bf-1), forebrain/midbrain (Otx2), midbrain/hindbrain (En2), GABAergic (GAD67), and medium spiny projection (DARPP-32) neurons, and astrocytes (GFAP) and oligodendrocytes (MBP). Scale bar: 50 μm. Otx2, orthodenticle homeobox 2; Bf-1, brain factor-1; Darpp-32, dopamine- and cAMP-regulated phosphoprotein, Mr 32 kDa; GABA, γ-aminobutyric acid; TH, tyrosine hydroxylase; GFAP, glial fibrillary acidic protein; O4; oligodendrocyte marker 4; En-1, engrailed-1; GAD67, glutamate decarboxylase 67; MBP, myelin basic protein.

transplanted cells forming astrocytes (GFAP) and oligodendrocytes (O4).

Recently it was reported that NPCs differentiated from mouse iPSCs can give rise to tumors when transplanted into a mouse model of MCAo (14), raising the safety concerns in using iPSC-NPCs for cell therapy in stroke. However, among the total of 20 cell transplanted and sham control groups in our study, we did not detect any signs of graft overgrowth or tumor formation. Contrary to the previous report of the mouse iPSCs, our NPC differentiation protocol may be more robust through a series of selection procedures and contain no undifferentiated cells. Alternatively, the intrinsic difference in mouse and human iPSCs in terms of neuronal differentiation may be attributed to the less tumorigenecity of human iPSC-derived NPCs. However, since 8 weeks of observation period may not be long enough to exclude the possibility of tumor formation, it may be necessary to monitor the tumor formation over more extended time periods such as six months or longer to ensure the safety of transplanted cells. Taken together, these results strongly suggest that 551-8 hiPSC-NPCs survive and contribute to the neural tissue formation and possibly neuronal regeneration in the infarct area without tumor formation.

In Vivo Tracking of 551-8 hiPSC-Derived NPCs Using Animal MRI

To monitor the fates of 551-8 cells following transplantation into the contralateral side of infarct area, we employed a 4.7-T animal MRI using T2 and T2*-weighted imaging techniques (Fig. 6A). Animal MRI was taken at 1 day after transplantation and right before sacrificing the animals after completion of behavior tests at 8 weeks posttransplantation. Figure 6A shows T2 and T2* images at 8 weeks following transplantation. Interestingly, we found that the great majority of transplanted cells migrate to the peri-infacrt area, exhibiting the patho-tropism of stem cells in stroke animal models. We have previously observed this phenomenon as well when BM-MSCs were used (16). More recently, similar phenomenon was also observed in our group when other cell types, such as human ESC-derived NPCs, neural stem cells (NSCs), and cord blood-derived MSCs, were transplanted and examined by MRI (data not shown). Importantly, we found that

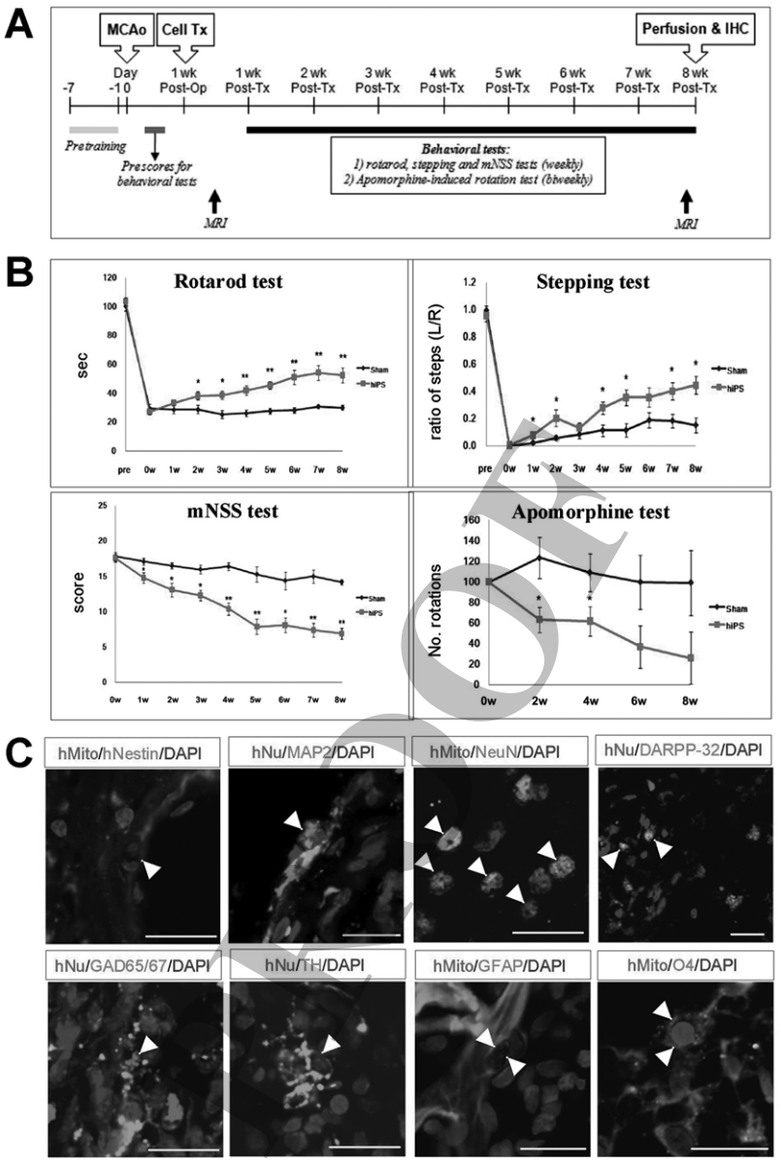

Figure 5. In vivo functional analyses of 551-8 hiPSC-derived NP cells following transplantation into a rodent model of MCAo. (A) Experimental scheme showing time schedules for making middle cerebral artery occlusion (MCAo) animal models and determination of prescores for behavioral tests (MCAo), cell transplantation (Cell Tx), posttransplantation follow-up studies including various behavioral tests (behavioral tests) and animal magnetic resonance imaging (MRI), followed by sacrifice of animals and histological analysis (perfusion and IHC). (B) Behavioral improvements following transplantation of 551-8 hiPSC-derived NP cells. Rotarod test, stepping test, and modified neurological severity score (mNSS) test were carried out every week, and apomorphine test was performed biweekly up to 8 weeks. $*p<0.05$; $**p<0.001$. w, week. (C) Immunohistochemical (IHC) staining to visualize the transplanted cells and their differentiated cell types. To detect the fate of transplanted cells, antibodies against either human-specific nuclei (hNu) or human-specific mitochondria (hMito) were used. Transplanted cells were shown to form human-specific NESTIN (hNESTIN), MAP2, neuronal nuclei (NeuN), DARPP-32, GAD65/67, TH, GFAP, and O4. DAPI was used to counterstain the cells. Arrows, colocalized marker expression. Scale bar: 20 μm.

the transplanted cells not only migrate tangentially across the brain hemisphere, mainly via corpus callosum, but also encompass the infarct area, judged by the widespread distribution of Feridex®-labeled cells in anterior to posterior position, regardless of injection site (Fig. 6A–C).

We also found that most of the migrated cells (80.10± 8.50%) express CXCR4 (Fig. 6C), the cognate receptor for the inflammatory chemoattractant SDF-1α (stromal cell-derived factor 1-α) that is known to be upregulated by local astrocytes and endothelium in response to ischemic

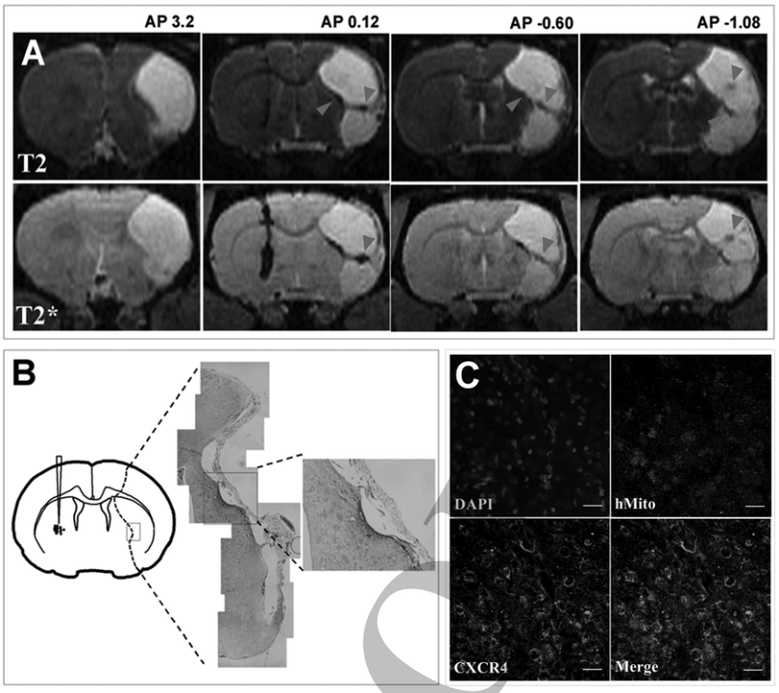

Figure 6. In vivo tracking of 551-8 hiPSC-derived neural precursor cells following transplantation into the contralateral side of infarct in a rodent model of MCAo. (A) 4.7T animal MRI analyses showing the coronal view of T2- and T2*-weighted images in antero-posterior sequences (from 4.2 to −1.20 mm, measured from the bregma). Note the migration of Feridex®-labeled transplanted cells to the infarct area (arrowheads). (B) Prussian blue staining showing the detection of Feridex®-labeled transplanted cells in the infarct area. (C) Immunocytochemical staining showing the presence of transplanted cells, judged by expression of human-specific mitochondria (hMito), which are also colocalized with chemokine (C-X-C motif) receptor 4 (CXCR4). Scale bar: 50 μm.

injury (11,22). Therefore, results from the animal MRI study and CXCR4 expression in transplanted cells from 551-8 NPCs strongly suggest that hiPSC-derived NPCs have the capacity to migrate to the injured brain, which fulfills the first critical step in stem cell homing and engraftment for tissue repair and regeneration.

Due to the limited accessibility to animal MRI facility, animal MRI was taken only twice in this experiment. But it will be more useful if MRI observation can be carried out routinely, so that selection of animals based on MRI-guided infarct volume measurement prior to transplantation, as well as more detailed follow-ups on the graft mobility or changes of infarct volume after transplantation, can be carried out.

Reduced Inflammation, Gliosis, and Apoptosis

Inflammation is a critical mediator of brain damage in response to ischemic injury. As demonstrated both in animal models (31) and human stroke patients (7), the post-ischemic inflammatory cascade involves a rapid activation of microglia and astrocytes. In this study, we first carried out quantitative analysis of two representative microglial markers, Iba-1 and ED1 expression in both iPSC-transplanted and sham control groups. While Iba-1 is expressed both in the ischemic core and the penumbra, ED1 is expressed in the ischemic core only (31). Penumbra is a region of constrained blood supply in which energy metabolism is preserved (9). Compared with the sham control, animals transplanted with 551-8 hiPSC-derived NPCs showed the significant reduction in the number of Iba-1$^+$ cells in the ischemic core ($53.40 \pm 4.66\%$ vs. $17.31 \pm 1.40\%$, $p < 0.05$) (Fig. 7A, first panel), although their difference in the penumbra was shown to be insignificant ($14.86 \pm 1.10\%$ vs.$12.51 \pm 1.27\%$, $p = 0.31$, figures not shown). Compared with the sham control, the number of round-shaped ED1-positive cells was also shown to be significantly reduced in the transplanted group ($23.84 \pm 2.71\%$ vs. $12.50 \pm 0.10\%$, $p < 0.05$) (Fig. 7A, second panel). Since this analysis was made 8 weeks following transplantation, it is currently unknown exactly when the reduction in inflammatory cells first occurred. However, it will be likely that this histological finding is the result of an earlier event (data not shown).

We also examined the number of astrocytes in both hiPSC-derived NPC-transplanted and sham control groups and found that GFAP-positive astrocytes in the

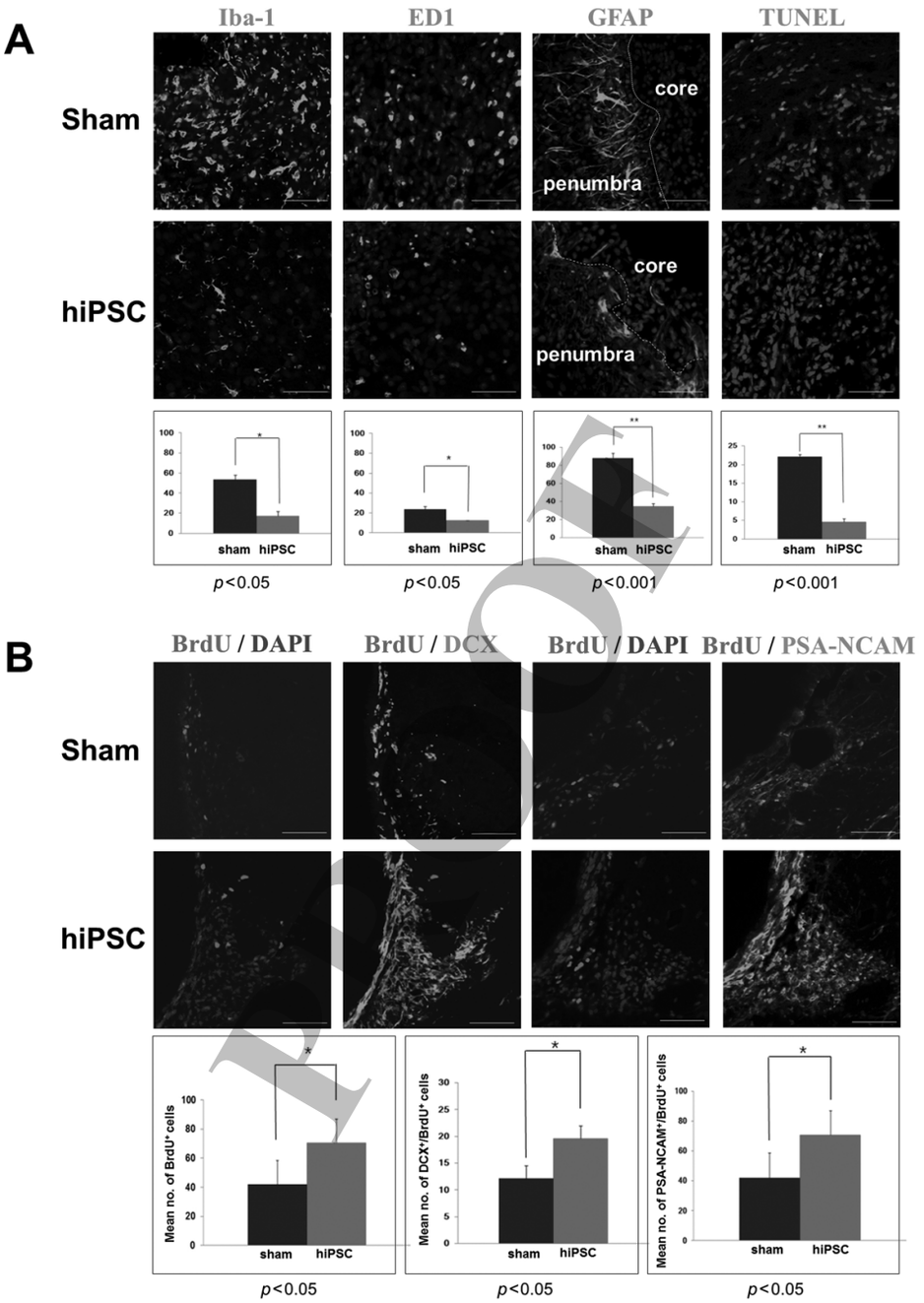

Figure 7. Transplantation effects of 551-8 hiPSC-derived NP cells. (A) Reduction of inflammation (Iba-1, ED1), gliosis (GFAP), and apoptosis (TUNEL) in transplanted animals, judged by immunohistochemical staining and cell counting, followed by statistical analysis. DAPI was used for counterstaining the cells. (B) Immunohistochemical staining showing the enhancement of endogenous neurogenesis (BrdU) and formation of migrating neuroblasts (DCX and PSA-NCAM) in the transplanted animals. Cell counting and statistical analysis was also performed. *$p<0.05$; **$p<0.001$. Scale bar: 50 μm. Iba-1, Ionized calcium binding adaptor molecule 1; ED1, antibody for cluster of differentiation 68 (CD68); TUNEL, Terminal deoxynucleotidyl transferase dUTP nick end labeling; BrdU, 5′-bromo-2′-deoxyuridine; DCX, doublecortin; PSA-NCAM, polysialylated neural cell adhesion molecule.

penumbra were greatly reduced in the transplanted group (87.70 ± 5.7% vs. 32.14 ± 3.53%, $p < 0.001$) (Fig. 7A, third panel). Proliferation of GFAP-positive astrocytes (gliosis) after ischemic injury usually leads to the formation of a glial scar. Therefore, it is likely that the transplanted iPSCs can also reduce the risk of glial scar formation. We also observed that the number of TUNEL-positive apoptotic cells was significantly reduced in the transplanted group (22.15 ± 0.60% vs. 4.59 ± 0.90%, $p < 0.001$) (Fig. 7A, last panel). At this stage, only few neurons undergo apoptosis as the major apoptotic events take place much earlier, during first 2 weeks after stroke. Therefore, it is likely that the TUNEL-positive cells are mostly represented by apoptotic microglia that might be involved in neural repair during later stages.

It is still controversial whether the activation of microglia and astrocytes are detrimental or beneficial to neuronal survival, neurogenesis, and functional recovery after stroke (6,12). Nevertheless, our results strongly suggest that the transplanted hiPSC-derived NPCs contribute to the reduction of inflammation, gliosis, and apoptosis in animal stroke model. Further study to understand how the transplanted cells play a role in each process at molecular levels will be important to optimize the use of hiPSC-derived NPCs for the treatment of stroke.

Promotion of Endogenous Neurogenesis Process

Stroke-induced neurogensis has been reported in adult brains, in which a pool of BrdU-positive endogenous NSCs or NPCs in the subventricular zone (SVZ) starts to proliferate and generate neuroblasts upon stroke-mediated injury (1). These newly generated neuroblasts have the capacity to migrate to the damaged area in the striatum and to differentiate into functional neurons (20,33). For this reason, it is now widely accepted that enhancement of endogenous neurogenesis would be one of most important targets for stroke therapeutics. Having this in mind, we addressed whether the transplanted hiPSC-derived NPCs have an influence on the endogenous neurogenesis. To do this, we injected the transplanted and sham control animals with BrdU three times at 12-h intervals prior to sacrifice. BrdU-positive cells were detected by immunohistochemistry using an antibody against BrdU, which were also double-stained with either DCX or PSA-NCAM, both of which are associated with neuronal migration.

While there was no difference of BrdU-positive cells in the contralateral side of SVZ between the iPSC-NPC transplanted and sham control groups (12.12 ± 2.39 vs. 19.56 ± 2.39, figures not shown), there was a significant difference in the ipsilateral side of SVZ (49.89 ± 7.03 vs. 83.83 ± 12.14, $p < 0.05$) (Fig. 7B) between them. Among the BrdU-positive cells, we found that significantly high numbers of cells positive for either DCX (12.17 ± 2.39 vs. 19.56 ± 2.39, $p < 0.05$) or PSA-NCAM (42.20 ± 16.38 vs. 70.67 ± 16.27, $p < 0.05$) were detected in the hiPSC-transplanted group, compared with the sham control. No BrdU-positive human cells were detected, meaning that the transplanted hiPSC-derived NPCs were unrelated to BrdU-positive cells. Taken together, these results strongly suggest that the transplanted hiPSC-derived NPCs greatly contribute to the proliferation of endogenous neural stem cells in the SVZ, as well as to their migration

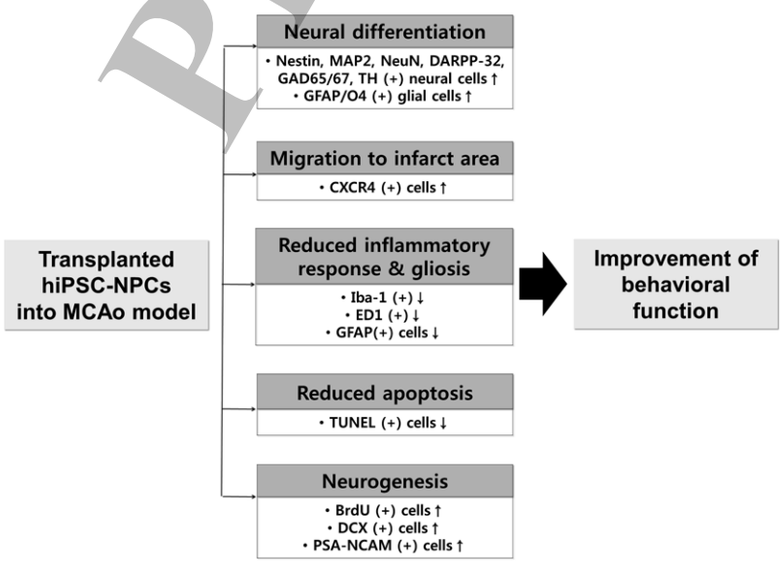

Figure 8. Schematic diagram showing the action mode of 551-8 hiPSC-derived NPCs following transplantation into MCAo animal models. See text for details.

to the infarct area in the striatum. However, although we observed a significant increase in SVZ cell proliferation and DCX-positive neuroblast formation, there was no evidence that DARPP-32-positive functional neurons were directly formed from endogenous neural stem cells. Therefore, it can be only said at this stage that the transplanted hiPSC-derived NPCs can promote some aspects of endogenous neurogenesis (i.e., proliferation and migration) but not the entire process (including mature neuron formation). How exactly the transplanted iPSC-NPCs can induce or mediate the enhancement of endogenous neurogenesis is currently unknown, but it will be likely that secretion of neurotrophic factors, modulation of inflammation, or promotion of angiogenesis by hiPSC-derived NPCs would play major roles in this process. For this, we have observed that several kinds of neurotrophic factors such as BDNF are highly expressed in the transplanted animals, as compared with sham controls (data now shown).

In summary, we have carried out the detailed analysis on the neurogenic and therapeutic potentials of NPCs derived from human iPSCs to treat stroke. Our results show that iPSCs can form NPCs efficiently and significant behavioral recovery can be achieved when these NPCs are transplanted into a rodent stroke model. As summarized in Figure 8, the transplanted hiPSC-derived NPCs led to not only behavioral recovery and neural tissue formation but also significant reduction in stroke-induced inflammatory response, gliosis, and apoptosis. More importantly, they contributed to the major events in endogenous neurogenesis. No tumor was found from the transplanted animals. So far, various types of stem cells have exhibited neurogenic and therapeutic potentials in animal models of stroke, but our work provides encouraging evidence showing that human hiPSC-derived NPCs have the capacity to cure the damaged brain by exerting three important modes of action simultaneously. Firstly, they migrate to the infarct area and form neural tissues in the stroke-damaged brain. Secondly, they reduce inflammation, gliosis, and apoptosis in the stroke-damaged brain. Thirdly, they contribute to the endogenous neurogenesis in the SVZ of stroke-induced brain. Although more evidence will be required to prove the effects of hiPSCs in neuronal restoration, neuroprotection, neural circuit connection, mature neuron formation, etc., given the importance of iPSCs as autologous sources for cell therapy, the current study provides the important possibility on the therapeutic potential of iPSCs in treating stroke. Obviously, it will be necessary to test multiple iPSC lines derived from viral or nonviral methods for the generalization of our results, and more extended follow-up study will be required to ensure the persistence and safety of transplantation effects.

ACKNOWLEDGMENTS: This work was supported by grants from the Korea Health Technology R&D Project, Ministry of Health and Welfare (A111016), the National Research Foundation of Korea (2010-0008719), and the Korea Food and Drug Administration (S-11-04-2-SJV-993-0-H), Republic of Korea to J.S. We are grateful to the MRI facility in the Division of Magnetic Resonance, Korea Basic Science Institute, Ochang, Korea. We also thank WiCell and RICKEN Cell Bank for providing us with H9 human ES cells and PA6 cells, respectively. J.S. is highly indebted to Professor Olle Lindvall who provided the initial support and the great inspiration on stroke research. The authors declare no conflicts of interest.

REFERENCES

1. Arvidsson, A.; Collin, T.; Kirik, D.; Kokaia, Z.; Lindvall, O. Neuronal replacement from endogenous precursors in the adult brain after stroke. Nat. Med. 8:963–970; 2002.
2. Bang, O. Y.; Lee, J. S.; Lee, P. H.; Lee, G. Autologous mesenchymal stem cell transplantation in stroke patients. Ann. Neurol. 57:874–882; 2005.
3. Bederson, J. B.; Pitts, L. H.; Tsuji, M.; Nishimura, M. C.; Davis, R. L.; Bartkowski, H. Rat middle cerebral artery occlusion: Evaluation of the model and development of a neurologic examination. Stroke 17:472–476; 1986.
4. Boulting, G. L.; Kiskinis, E.; Croft, G. F.; Amoroso, M. W.; Oakley, D. H.; Wainger, B. J.; Williams, D. J.; Kahler, D. J.; Yamaki, M.; Davidow, L.; Rodolfa, C. T.; Dimos, J. T.; Mikkilineni, S.; MacDermott, A. B.; Woolf, C. J.; Henderson, C. E.; Wichterle, H.; Eggan, K. A functionally characterized test set of human induced pluripotent stem cells. Nat. Biotechnol. 29:279–286; 2011.
5. De Ryck, M.; Van Reempts, J.; Borgers, M.; Wauquier, A.; Janssen, P. A. Photochemical stroke model: Flunarizine prevents sensorimotor deficits after neocortical infarcts in rats. Stoke 20:1383–1390; 1989.
6. Ekdahl, C. T.; Kokaia, Z.; Lindvall, O. Brain inflammation and adult neurogenesis: The dual role of microglia. Neuroscience 158:1021–1029; 2009.
7. Gerhard, A.; Neumaier, B.; Elitok, E.; Glatting, G.; Ries, V.; Tomczak, R.; Ludolph, A. C.; Reske, S. N. In vivo imaging of activated microglia using [11C]PK11195 and positron emission tomography in patients after ischemic stroke. Neuroreport 11:2957–2960; 2000.
8. Honmou, O.; Houkin, K.; Matsunaga, T.; Niitsu, Y.; Ishiai, S.; Onodera, R.; Waxman, S. G.; Kocsis, J. D.Intravenous administration of auto serum-expanded autologous mesenchymal stem cells in stroke. Brain 134:1790–1807; 2011.
9. Hossmann, K. A. Pathophysiology and therapy of experimental stroke. Cell. Mol. Neurobiol. 26:1057–1083; 2006.
10. Hu, B. Y.; Weick, J. P.; Yu, J.; Ma, L. X.; Zhang, X. Q.; Thomson, J. A.; Zhang, S. C. Neural differentiation of human induced pluripotent stem cells follows developmental principles but with variable potency. Proc. Natl. Acad. Sci. USA 107:4335–4340; 2010.
11. Imitola, J.; Raddassi, K.; Park, K. I.; Mueller, F. J.; Nieto, M.; Teng, Y. D.; Frenkel, D.; Li, J.; Sidman, R. L.; Walsh, C. A.; Snyder, E. Y.; Khoury, S. J. Directed migration of neural stem cells to sites of CNS injury by the stromal cell-derived factor 1 α/CXC chemokine receptor 4 pathway. Proc. Natl. Acad. Sci. USA 101:18117–122; 2004.
12. Jablonska, A.; Lukomska, B. Stroke induced brain changes: Implications for stem cell transplantation. Acta Neurobiol. Exp. 71:74–85; 2011.

13. Jeong, S. W.; Chu, K.; Jung, K. H.; Kim, S. U.; Kim, M.; Roh, J. K. Human neural stem celltransplantation promotes functional recovery in rats with experimental intracerebral hemorrhage. Stroke 34:2258–2263; 2003.
14. Kawai, H.; Yamashita, T.; Ohta, Y.; Deguchi, K.; Nagotani, S.; Zhang, X.; Ikeda, Y.; Matsuura, T.; Abe, K. Tridermal tumorigenesis of induced pluripotent stem cells transplanted in ischemic brain. J. Cereb. Blood Flow Metab. 30:1487–1493; 2010.
15. Kawasaki, H.; Mizuseki, K.; Nishikawa, S.; Kaneko, S.; Kuwana, Y.; Nakanishi, S.; Nishikawa, S. I.; Sasai, Y. Induction of midbrain dopaminergic neurons from ES cells by stromal cell-derived inducing activity. Neuron 28:31–40; 2000.
16. Kim, D.; Chun, B. G.; Kim, Y. G.; Lee, Y. H.; Park, C. S.; Jeon, I.; Cheong, C.; Hwang, T. S.; Chung, H.; Gwag, B. J.; Hong, K. S.; Song, J. In vivo tracking of human mesenchymal stem cells in experimental stroke. Cell Transplant. 16:1007–1012; 2008.
17. Kondziolka, D.; Steinberg, G.K.; Wechsler, L.; Meltzer, C. C.; Elder, E.; Gebel, J.; Decesare, S.; Jovin, T.; Zafonte, R.; Lebowitz, J.; Flickinger, J. C.; Tong, D.; Marks, M. P.; Jamieson, C.; Luu, D.; Bell-Stephens, T.; Teraoka, J. Neurotransplantation for patients with subcortical motor stroke: A phase 2 randomized trial. J. Neurosurg. 103:38–45; 2005.
18. Kondziolka, D.; Wechsler, L.; Goldstein, S.; Meltzer, C.; Thulborn, K.R.; Gebel, J.; Jannetta, P.; DeCesare, S.; Elder, E. M.; McGrogan, M.; Reitman, M. A.; Bynum, L. Transplantation of cultured human neuronal cells for patients with stroke. Neurology 55:565–569; 2000.
19. Lindvall, O.; Kokaia, Z. Stem cell research in stroke: How far from the clinic? Stroke 42(8):2369–2375; 2011.
20. Lindvall, O.; Kokaia, Z. Stem cells in human neurodegenerative disorders—time for clinical translation? J. Clin. Invest. 120:29–40; 2010.
21. Longa, E. Z.; Weinstein, P. R.; Carlson, S.; Cummins, R. Reversible middle cerebral artery occlusion without craniectomy in rats. Stroke 20:84–91; 1989.
22. Miller, R. J.; Banisadr, G.; Bhattacharyya, B. J. CXCR4 signaling in the regulation of stem cell migration and development. J. Neuroimmunol. 198;31–38; 2008.
23. Nelson, P. T.; Kondziolka, D.; Wechsler, L.; Goldstein, S.; Gebel, J.; DeCesare, S.; Elder, E. M.; Zhang, P. J.; Jacobs, A.; McGrogan, M.; Lee, V. M.; Trojanowski, J. Q. Clonal human (hNT) neuron grafts for stroke therapy: Neuropathology in a patient 27 months after implantation. Am. J. Pathol. 160:1201–1206; 2002.
24. Olsson, M.; Nikkhah, G.; Bentlage, C.; Björklund, A. Forelimb akinesia in the rat Parkinson model: Differential effects of dopamine agonists and nigral transplants as assessed by a new stepping test. J. Neurosci. 15:3863–3875; 1995.
25. Osafune, K.; Caron, L.; Borowiak, M.; Martinez, R. J.; Fitz-Gerald, C. S.; Sato, Y.; Cowan, C. A.; Chien, K. R.; Melton, D. A. Marked differences in differentiation propensity among human embryonic stem cell lines. Nat. Biotechnol. 26:313–315; 2008.
26. Park, I. H.; Arora, N.; Huo, H.; Maherali, N.; Ahfeldt, T.; Shimamura, A.; Lensch, M. W.; Cowan, C.; Hochedlinger, K.; Daley, G. Q. Disease-specific induced pluripotent stem cells. Cell 134:877–886; 2008.
27. Park, I. H.; Lerou, P. H.; Zhao, R.; Huo, H.; Daley, G. Q. Generation of human-induced pluripotent stem cells. Nat. Protoc. 3:1180–1186; 2008.
28. Park, I. H.; Zhao, R.; West, J. A.; Yabuuchi, A.; Huo, H.; Ince, T. A.; Lerou, P. H.; Lensch, M. W.; Daley, G. Q. Reprogramming of human somatic cells to pluripotency with defined factors. Nature 451:141–146; 2008.
29. Pollock, K.; Stremer, P.; Patel, S.; Stevanato, L.; Hope, A.; Miljan, E.; Dong, Z.; Hodges, H.; Price, J.; Sinden, J. D. A conditionally immortal clonal stem cell line from human cortical neuroepithelium for the treatment of ischemic stroke. Exp. Neurol. 199:143–155; 2006.
30. Reglodi, D.; Tamás, A.; Lengvári, I. Examination of sensorimotor performance following middle cerebral artery occlusion in rats. Brain Res. Bull. 59:459–466; 2003.
31. Schilling, M.; Besselmann, M.; Leonhard, C.; Mueller, M.; Ringelstein, E. B.; Kiefer, R. Microglial activation precedes and predominates over macrophage infiltration in transient focal cerebral ischemia: A study in green fluorescent protein transgenic bone marrow chimeric mice. Exp. Neurol. 183:25–33; 2003.
32. Ungerstedt, U.; Arbuthnott, G. W. Quantitative recording of rotational behavior in rats after 6-hydroxydopamine lesions of the nigrostriatal dopamine system. Brain Res. 24:485–493; 1970.
33. Zhang, Z. G.; Chopp, M. Neurorestorative therapies for stroke: Underlying mechanisms and translation to the clinic. Lancet Neurol. 8:491–500; 2009.